

## Responses to the Editor

*Initial comments in red italics*, responses in plain text

*I would like to thank you for your careful revisions. However, I think there are some additional revisions necessary. First of all, I would strongly recommend to find a native speaker to proofread your manuscript. There are many examples of linguistic defficiencies and grammatical inconsistencies. Furthermore, I would suggest strongly to include a map showing all the cave sites used for this study.*

- 1) Dr. Nick Belshaw, a native speaker, from Earth Science Department, Oxford University, helped with the manuscript proofreading. And all corrections are shown in the marked-up manuscript version. The deleted words are shown as blue-colored texts with a line in the middle, while the inserted words are shown as red-colored texts.
- 2) A map with all the cave sites used for this study has been included in the revised manuscript shown as Fig. 1.

# Quantification of southwest China rainfall during the 8.2 ka BP event with response to North Atlantic cooling

Y. Liu<sup>1,2</sup>, C. Hu<sup>1</sup>

<sup>1</sup> State key lab of biogeology and environmental geology, China University of Geosciences, Wuhan, 430074, PR China

<sup>2</sup> Faculty of Materials Science & Chemistry, China University of Geosciences, Wuhan, 430074, PR China

*Correspondence to:* Y. Liu (yhliu@cug.edu.cn)

**Abstract.** The 8.2 ka BP event could provide important information for predicting abrupt climate change in the future. Although published records show that the East Asian monsoon area responded to the 8.2 ka BP event, there is no high resolution quantitative reconstructed climate record in this area. In this study, a reconstructed 10-yr moving average annual rainfall record in southwest China during the 8.2 ka BP event is presented by comparing two high-resolution stalagmite  $\delta^{18}\text{O}$  records from Dongge cave and Heshang cave. This decade-scale rainfall reconstruction is based on a central-scale model and is confirmed by inter-annual monitoring records, which shows a significant positive correlation between the regional mean annual rainfall amount and the drip water annual average  $\delta^{18}\text{O}$  difference from two caves along the same monsoon moisture transport pathway from May 2011 to April 2014. Similar trends between the reconstructed rainfall and the stalagmite Mg/Ca record, another proxy of rainfall, during the 8.2 ka BP period further increase the confidence of the quantization of the rainfall record. The reconstructed record shows that the mean annual rainfall in southwest China during the central 8.2 ka BP event is less than that of present (1950 ~ 1990) by ~200 mm, and decreased by ~350 mm in ~70 years experiencing an extreme drying period lasting for ~50 years. Further analysis on Comparison of the reconstructed rainfall record in southwest China and with Greenland ice core  $\delta^{18}\text{O}$  with and  $\delta^{15}\text{N}$  records, suggests that the reduced rainfall decrease in southwest China during the 8.2 ka BP period was coupled with Greenland cooling with a possible response rate of  $110 \pm 30 \text{ mm}/^\circ\text{C}$ .

## 1 Introduction

As evidence in support of global warming becomes stronger, it is apparent that the anticipated rise in sea levels may be higher than expected (Rahmstorf, 2007) and the frequency and amplitude of abrupt climate change (Martrat et al., 2004; Pall et al., 2007) may also be greater. As climate events are likely to be problematic for both ecosystems (Walther et al., 2002) and human society (Khasnis and Nettleman, 2005), any aid in prediction is crucial.

Studies of past climate events could hopefully provide useful information for exploring trigger mechanisms (Cheng, et al., 2009; Liu et al, 2013). The 8.2 ka BP event is noted to be the most pronounced abrupt climate event occurring during the whole Holocene (Alley and Ágústsson, 2005). The highest magnitude variation across the low to high latitudes makes a viable target for numerical modelings (Daley et al, 2011; Morrill et al., 2011) and may offer an insight into the sensitivity of

38 climate response in different areas (Condrón and Winsor, 2011; LeGrand and Schmidt,  
39 2008). This event was firstly identified in Greenland ice cores (Alley et al., 1997),  
40 showing a duration of 160-yr (Thomas et al., 2007) with a temperature drop of  $3.3 \pm 1.1$  °C  
41 in central Greenland (Kobashi et al., 2007), and is known globally (Dixit et al., 2014;  
42 Morrill et al., 2013; Ljung et al., 2008; Ellwood and Gose, 2006). However, as most  
43 records associated with this event mainly derived from North Atlantic and Europe  
44 (Daley et al., 2011; Szeroczyńska and Zawisza, 2011; Snowball et al., 2010; Hede et  
45 al., 2010; Domínguez-Villar et al., 2009; Prasad et al., 2009), the question remains as  
46 to how much it influenced the East Asian monsoon area (EAMA).

47 Although some proxies from lake sediments (Yu et al., 2006; Hong et al., 2009;  
48 Zheng et al., 2009; Mischke and Zhang, 2010), stalagmites (Wu et al., 2012; Cheng et  
49 al., 2009; Hu et al., 2008a; Wang et al., 2005; Dykoski et al., 2005) and marine  
50 sediments (Zheng et al., 2010; Ge et al., 2010) do record the 8.2 ka BP event in  
51 EAMA, only Hu et al. (2008a) attempted a quantitative reconstruction of rainfall by  
52 using stalagmite  $\Delta\delta^{18}\text{O}$  records which indicated a decrease in precipitation during the  
53 event in southwest China, an area influenced by East Asian monsoon. However, the  
54 resolution of this precipitation record is approximately 100-yr and needs to be  
55 improved.

56 Based on the method presented by Hu et al. (2008a), this study reconstructs a 10-yr  
57 averaged annual rainfall record in southwest China during the 8.2 ka BP event by  
58 comparing sub-annual (Liu et al., 2013) and 3.5-yr resolution stalagmite  $\delta^{18}\text{O}$  (Cheng  
59 et al., 2009) records from the same moisture transport pathway. This study further  
60 addresses the sensitivity of the climate of southwest China to North Atlantic cooling  
61 during the 8.2 ka BP event, providing quantitative data for simulating this global  
62 event in climate system models.

## 63 2 Methods

### 64 2.1 Rainfall reconstruction

65 It has been previously discussed (Hu, et al., 2008a) that, in a monsoon area, regional  
66 rainfall histories could be reconstructed by using coeval stalagmite  $\delta^{18}\text{O}$  comparisons  
67 between two close sites located along the same atmospheric moisture transport  
68 pathway, as the difference allows the removal of secondary controls, such as moisture  
69 transport and temperature on  $\delta^{18}\text{O}$ . Working with this premise, two published high  
70 resolution stalagmite  $\delta^{18}\text{O}$  sequences during the 8.2 ka BP event from Heshang cave,  
71 central China (Liu et al., 2013) and Dongge cave, southwest China (Cheng et al.,  
72 2009), located directly upstream in the atmospheric pathway (Fig. 1), were investigated.

#### 73 2.1.1 Stalagmite $\Delta\delta^{18}\text{O}$ sequence establishment

74 There is only one high-resolution  $\delta^{18}\text{O}$  record produced by from stalagmite HS4 from  
75 in Heshang cave (30°27'N, 110°25'E) (Fig. 1), central China, covering the 8.2 ka  
76 BP period (Liu et al., 2013), with an average resolution of ~0.3-yr. However, there are

77 two published stalagmite  $\delta^{18}\text{O}$  records (stalagmite DA and D4) from Dongge cave  
78 (25°17'N, 108°5'E)(Fig.1), southwest China (Wang et al., 2005; Dykoski et al., 2005).  
79 Since Cheng et al.(2009) re-dated both DA and D4 from Dongge cave across during  
80 the 8.2 ka BP period to obtain produce a better controlled chronology, both DA and  
81 D4 giving  $\delta^{18}\text{O}$  records with an average resolution of ~3.5-yr and ~2-yr (Cheng et al.,  
82 2009) respectively. These records are then compared with HS4 using the approach  
83 outlined in Hu et al. (2008a).

84 It may be observed that Fig. 2 shows the  $\delta^{18}\text{O}$  records from HS4 (Fig.21a) (Liu et  
85 al., 2013), DA (Fig. 21b) and D4 (Fig. 21c) (Cheng et al., 2009) show where similar  
86 structural patterns are observed with matching major peaks and troughs. Typical  
87 corresponding peaks or troughs are then marked as shown by dashed lines in Fig. 21  
88 and the chronology of DA, D4 and HS4 are so matched to reduce the chronologically  
89 uncertainty. It should be noted that the wiggle matching is within the analytical  
90 uncertainty of the U-Th chronology. As the measurement resolutions of HS4, DA and  
91 D4 are different, all the sequences were first processed to create records of equivalent  
92 annual resolution and allowing the resultant time sequences, then to be used to  
93 construct a 10-yr moving average sequence. Two new  $\delta^{18}\text{O}$  difference ( $\Delta\delta^{18}\text{O}$ )  
94 sequences between HS4 and adjusted DA records (Fig. 21d) and between HS4 and  
95 adjusted D4 records (Fig. 21e) were thus established.

96 Though there is a systematic offset between Fig. 21d and Fig. 21e, generally the  
97 variations and trends of the two sequences are similar, suggesting either of the two  
98  $\Delta\delta^{18}\text{O}$  sequences could be used for the following reconstruction. Since the  $\delta^{18}\text{O}$   
99 record from Dongge cave adopted in Hu et al.(2008a) is from DA, in this study also  
100 uses data from DA  $\Delta\delta^{18}\text{O}$  from (Fig. 21d) is used for further rainfall reconstruction.

### 101 2.1.2 Uncertainties of $\Delta\delta^{18}\text{O}$

102 Since the use of  $\Delta\delta^{18}\text{O}$  sequence is intending to reconstruct the regional rainfall  
103 quantitatively, it is necessary to assess requires some understanding of the  
104 uncertainties of within the measurement records and calculations. The first need to be  
105 taken into consideration is the chronology uncertainty. As the U/Th dating maximum  
106 uncertainty of stalagmite DA during the 8.2 ka BP period is 94 ~90-yr (Cheng et al.,  
107 2009) and, while the average difference between the adjusted and original DA data set  
108 to match HS4 is ~40-yr. This adjustment is within the dating uncertainty, but to test  
109 the robustness of the approach, is tested by shifting the whole DA  $\delta^{18}\text{O}$  data set is  
110 shifted by 50-yr young and 50-yr in both older and younger directions respectively  
111 and the resultant data sets are compared. These three  $\Delta\delta^{18}\text{O}$  sequences are shown in  
112 Fig. 32a along with unchanged DA chronology (in-black), shifting DA 50-yr younger  
113 (in-blue) and 50-yr older (in-red). Fig. 32a demonstrates suggests that though the time  
114 shifted chronology data sets do show increased variability the uncertainty of the  
115  $\Delta\delta^{18}\text{O}$  with a maximum error of 0.76‰, the general variation trends are similar,  
116 suggesting indicating that this difference method is sufficiently accurate-robust for  
117 this study.

118 ~~Besides~~In addition to the chronology uncertainty, other factors may affect the  
119 ~~uncertainty accuracy~~ of  $\Delta\delta^{18}\text{O}$ . ~~Firstly, it is from the~~ $\delta^{18}\text{O}$  analytical uncertainties  
120 ~~from of the~~ HS4 and DA ~~datasets, which~~ are 0.08‰ (Liu et al. 2013) and 0.15‰  
121 (Cheng, et al., 2009) respectively. ~~Secondly, it is from~~Additionally the standard  
122 deviation of the 10-yr average, ~~and especially~~ the largest standard deviation of  $\Delta\delta^{18}\text{O}$   
123 between DA and HS4 is 0.62‰. ~~Also, there is~~And an estimated uncertainty of 0.35‰  
124 from the model established by Hu et al. (2008a) ~~should be noted~~. Taking all of these  
125 factors into consideration, the final uncertainty of the  $\Delta\delta^{18}\text{O}$  sequence during the 8.2  
126 ka BP period ~~could be~~is estimated to be ~0.53‰.

### 127 2.1.3 Rainfall reconstruction

128 Based on the  $\Delta\delta^{18}\text{O}$  sequence shown in Fig. 32b, the ~~quantitative~~ rainfall  
129 ~~reconstruction~~ during the 8.2 ka BP period ~~could be built by~~is reconstructed using the  
130 previous model presented by Hu et al. (2008a), ~~as the established model covering the~~  
131 ~~8.2-ka BP period. The~~via the relation between  $\Delta\delta^{18}\text{O}$  and rainfall  
132 ( $\text{Rainfall}=189.08\times\Delta\delta^{18}\text{O}+1217.4$ ) (Hu et al., 2008a) ~~is therefore considered suitable~~  
133 ~~for this study. And~~The uncertainties from  $\Delta\delta^{18}\text{O}$  ~~would~~ give an ~~uncertainty error~~ of  
134 ~100 mm/yr for the reconstructed rainfall record.

135 ~~The idea of~~Reconstructing of regional rainfall ~~between two caves by comparing~~  
136 using two spatially separated cave records ~~along on~~ the same moisture transport  
137 pathway ~~is to presume single~~requires stalagmite  $\delta^{18}\text{O}$  values from monsoon areas ~~at~~  
138 ~~least contain to faithfully preserve~~ rainfall information. ~~For Chinese~~stalagmite  $\delta^{18}\text{O}$   
139 values, ~~they~~ are ~~indeed~~ influenced by different types of precipitation, ~~and as well as~~  
140 ~~moisture along with the~~ source and ~~its~~ pathways of moisture, plus local condensation  
141 and evaporation processes (Dayem et al., 2010). ~~And a~~ recent millennial scale climate  
142 simulation (Liu et al., 2014) ~~also~~ suggests that Chinese stalagmite  $\delta^{18}\text{O}$  records ~~could~~  
143 ~~be used might be useful~~ as ~~an~~ indicators of intensity of the East Asian summer  
144 monsoon in terms of the continental scale Asian monsoon rainfall response in the  
145 upstream regions ~~(Liu et al., 2014)~~. As both Dongge and Heshang  $\delta^{18}\text{O}$  records  
146 respond to ~~the~~ upstream rainfall ~~respectively~~, the difference of the two records ~~should~~  
147 ~~be related is expected to directly reflect~~ the ~~regional~~ rainfall between Dongge and  
148 Heshang ~~cave~~.

149 ~~Since~~On decadal scale, ~~the~~ relationships between  $\Delta\delta^{18}\text{O}$  and rainfall ~~records was~~  
150 ~~confirmed have previously been discussed~~ (Hu et al., 2008a), ~~and we~~ here ~~we further~~  
151 ~~access attempt to utilize this method approach~~ on an inter-annual time scale.  
152 ~~Compared with local precipitation~~  $\delta^{18}\text{O}$  ( $\delta^{18}\text{O}_p$ ), ~~an outside cave signal, monitoring A~~  
153 ~~direct test of the validity of using moisture transport pathways would use~~ cave drip  
154 water  $\delta^{18}\text{O}$  ( $\delta^{18}\text{O}_d$ ) signals from both DA and HS4 sites ~~which~~ should reflect  
155 speleothem  $\delta^{18}\text{O}$  variations ~~more~~ directly. ~~Though~~ Unfortunately there is no published  
156 monitoring data from Dongge, ~~However~~ there ~~are is~~ some ~~latest recently~~ published  
157 ~~cave monitoring~~  $\delta^{18}\text{O}_d$  data from a cave named Liangfeng (26°16'N, 108°03'E) (Fig. 1)  
158 ~~between from~~ May 2011 ~~and to~~ April 2014 with local precipitation  $\delta^{18}\text{O}$  ( $\delta^{18}\text{O}_p$ ) data  
159 (Duan et al., 2016) ~~from a cave named Liangfeng (26°16'N, 108°03'E)~~. Liangfeng is  
160 close to Dongge (25°17'N, 108°5'E) (Fig. 1) and may therefore, ~~which might~~ be an

161 alternative **data source** to assess the **validity of the** rainfall reconstruction method.

162 There are three separate sequences of  $\delta^{18}\text{O}_d$  from different dripping sites in  
163 Liangfeng cave (Zeng et al, 2015). **Among-From** them, LF6  $\delta^{18}\text{O}_d$ -with **a-the** lowest  
164 drip rate but highest variation-**amplitude** has been selected, as it **may-is considered to**  
165 record climate information more efficiently. The lowest drip rate of LF6 from  
166 Liangfeng cave **indicates-suggests** fresh water **is being** mixed with **more-delayed**  
167 **transit** stored water for this dripping site (Zeng et al, 2015), **which-and** may provide  
168 longer term instead of **short** seasonal information compared with the other two sites.  
169 Based on the **3-yr-years** of monthly monitoring data of LF6 and HS4 (Duan et al.,  
170 2016), the sequences of annual moving average  $\delta^{18}\text{O}_d$  of LF6 and HS4 have been  
171 **established-respectively-calculated**. Generally LF6  $\delta^{18}\text{O}_d$  values are higher than **those**  
172 **of** HS4- $\delta^{18}\text{O}_d$ , which is sensible since Heshang cave is further along the moisture  
173 transport pathway(**Fig.1**). **Since-LF6**  $\delta^{18}\text{O}_d$  is **considered** mixed **by** fresh and stored  
174 water, **so** its response to the local rainfall **may-is expected to** be delayed. **As there is-a**  
175 **A calculated** positive correlation( $R^2=0.62$ ) between the local annual moving average  
176  $\delta^{18}\text{O}_p$  and the 2-month delayed annual moving average of LF6  $\delta^{18}\text{O}_d$  (**monthly**  $\delta^{18}\text{O}_p$   
177 **and**  $\delta^{18}\text{O}_d$  data are from Duan et al., 2016), **it-is presumed-strongly suggests** that **LF6**  
178  $\delta^{18}\text{O}_d$ -**may-be-a** delayed **by-of** 2 months **should be applied when using LF6**  $\delta^{18}\text{O}_d$  data.  
179 **And-the same similar** analysis **on-of**  $\delta^{18}\text{O}_d$  at HS4 site and  $\delta^{18}\text{O}_p$  outside Heshang cave  
180 (Duan et al., **2015-2016**) reveals a positive correlation( $R^2=0.71$ ) between the local  
181 annual moving average  $\delta^{18}\text{O}_p$  and **the-a** 4-month delayed annual moving average **of**  
182 **for** HS4  $\delta^{18}\text{O}_d$ . **Further-Combined** analysis shows a positive correlation ( $R^2=0.72$ )  
183 between the 2-month delayed annual moving average of LF6  $\delta^{18}\text{O}_d$  and the 4-month  
184 delayed annual moving average of HS4  $\delta^{18}\text{O}_d$ , **indicating-the-main-giving some**  
185 **support to the idea that the controlling** factors-**controlled** on both LF6 and HS4  $\delta^{18}\text{O}_d$   
186 **values-should-be-are** similar, **so it is sensible to use their**  $\Delta\delta^{18}\text{O}_d$ -**records to discuss the**  
187 **efficiency of the rainfall reconstruction method**.

188 After the **time adjusted annual moving average**- $\Delta\delta^{18}\text{O}_d$  sequence **between 2 month**  
189 **delayed LF6**  $\delta^{18}\text{O}_d$  **and 4 month delayed HS4**  $\delta^{18}\text{O}_d$ -has been built, the correlation  
190 between  $\Delta\delta^{18}\text{O}_d$  and the regional average annual rainfall **amount-from-at** six sites  
191 between Dongge cave and Heshang cave **mentioned-detailed** in Hu et al. (2008a)(**Fig.**  
192 **1**) **could-may** be **analyzed-compared**. The regional average annual rainfall **amount** is  
193 calculated from monthly instrumental records between May 2011 and April 2014  
194 from <http://www.wunderground.com/history/>. **Fig. 43** shows that there is a significant  
195 positive correlation ( $R^2=0.79$ ) between annual **average**  $\Delta\delta^{18}\text{O}_d$  and regional annual  
196 rainfall **amount**. **The significant correlation further**, **supportings** the idea that the  
197 stalagmite  $\Delta\delta^{18}\text{O}$  between two caves located along the same moisture transport  
198 pathway **could-reveal-the can provide information on** regional rainfall variation, **since**  
199 **stalagmite**  $\delta^{18}\text{O}$  **derives from the drip water**  $\delta^{18}\text{O}$ .

## 200 2.2 Mg/Ca data processing

201 In addition to  $\Delta\delta^{18}\text{O}$ , the Mg/Ca ratio, another important rainfall proxy, **is can be**



202 considered ~~in this paper~~. The Mg/Ca data set is taken from Liu et al. (2013) measured  
203 ~~by using~~ a JEOL JXA8800R Electron Microprobe at the Department of Material  
204 Sciences, Oxford, along the HS4 stalagmite growth axis. The Mg/Ca data were  
205 processed to provide annual resolution and a 10-yr moving average constructed in the  
206 same way as for  $\delta^{18}\text{O}$ .

### 207 3 Results

208 The 10-yr moving average  $\Delta\delta^{18}\text{O}$  records ~~between from~~ DA and HS4 is shown in Fig.  
209 32b. It is reasonable that the DA  $\delta^{18}\text{O}$  values are generally higher than those of HS4  
210 (Fig. 21a and Fig. 21b) ~~as since~~ Heshang Cave is located further along the moisture  
211 transport pathway (Fig. 1), ~~which produces and is so expected to displayed a~~  
212 systematic  $\delta^{18}\text{O}$  offset. ~~Compared with an~~ The average  $\delta^{18}\text{O}$  difference ~~between HS4~~  
213 ~~and DA is of~~ 1.0‰ (Hu, et al, 2008) ~~between HS4 and DA~~ during the whole Holocene  
214 (Hu, et al, 2008), while the average  $\Delta\delta^{18}\text{O}$  value during the 8.2 ka BP event shown in  
215 Fig. 32b is much lower, ~~only with a value of at~~ 0.26‰.

216 ~~It may be observed in Fig. 2b that d~~ During the central event, it is notable that some  
217 of the  $\Delta\delta^{18}\text{O}$  values are around zero or even negative, indicating much reduced  
218 moisture transport during that time. While the lowest value of  $\Delta\delta^{18}\text{O}$  is nearly -0.50‰  
219 (Fig. 32b), we do not expected negative  $\Delta\delta^{18}\text{O}$  values. ~~Besides t~~ The estimated  
220 uncertainty of ~0.53‰ ~~produced by in~~ the  $\Delta\delta^{18}\text{O}$  ~~mentioned detailed in section 2.1.2,~~  
221 ~~along with the~~ difference in evaporation in the two caves is likely to contributes to  
222 ~~producing a the~~ negative  $\Delta\delta^{18}\text{O}$  ~~as well. Actually e~~ Cave monitoring data ~~do~~  
223 suggest evaporation may occur during the dripping and ~~exuding enhanced~~  
224 in a dry season could result in heavier drip water  $\delta^{18}\text{O}$  values (Zeng et al., 2015), ~~so~~  
225 ~~evaporation must result in heavier stalagmite  $\delta^{18}\text{O}$  values during dry period,~~  
226 especially in a well ventilated cave.

227 ~~Compared with~~ Dongge is, a cave consisting of branches with twists and turns, ~~the~~  
228 ~~structure of while~~ Heshang is a much simpler cave ~~is much simpler only~~ with a nearly  
229 straight main passage, and ~~with a~~ 20 m high entrance (Hu et al., 2008b). ~~So~~ Heshang  
230 cave is ~~clearly much~~ more open and better ventilated than Dongge cave, ~~and indeed it~~  
231 ~~leadings to an obvious greater~~ heat and moisture exchange between the inside and  
232 outside cave (Hu et al, 2008b). ~~Therefore on~~ During similar dry conditions, the  
233 evaporation effects in Heshang cave are expected to be ~~is much~~ more significant than  
234 in Dongge Cave, and the drier the condition ~~it is,~~ the heavier HS4  $\delta^{18}\text{O}$  values  
235 ~~expected would be,~~ leading to lower or even negative  $\Delta\delta^{18}\text{O}$  values between DA and  
236 HS4. ~~That means Thus~~ less rainfall is still related to lower  $\Delta\delta^{18}\text{O}$  values ~~with the~~  
237 ~~consideration of cave evaporation effect~~. Since the 8.2 ka BP event is the driest period  
238 during the whole Holocene (Hu et al., 2008), negative  $\Delta\delta^{18}\text{O}$  values produced during  
239 the central event ~~is are~~ possible.

240 From the 10-year moving average  $\Delta\delta^{18}\text{O}$  ~~between the~~ obtained from HS4 and DA  
241 records (Fig. 32b), there is a significant change in value ~~by 1.8‰~~ from 1.3‰ to -0.5‰  
242 ~~over approximately happened in ~70 years at the beginning commencement~~ of the

243 event. Compared with the average amplitude of  $\Delta\delta^{18}\text{O}$  during the whole Holocene of  
244 1.0‰ (Hu et al., 2008a), ~~during the 8.2 ka BP period, the  $\delta^{18}\text{O}$  value drops greatly and~~  
245 ~~the amplitude is nearly doubled~~ **this is a surprisingly large change.**

246 ~~Based on~~ **From** the  $\Delta\delta^{18}\text{O}$  record shown in Fig.32b, using the previously  
247 determined relation (Rainfall=189.08 $\times\Delta\delta^{18}\text{O}$  +1217.4) ~~published in~~ **from** Hu et al.  
248 (2008a), the rainfall record in southwest China during the 8.2 ka BP period ~~could~~ **may**  
249 be established as shown in Fig.32b. ~~Besides the~~ **While** some support for the  
250 reconstruction method **can be obtained using recent** ~~by~~ monitoring records ~~shown~~  
251 ~~detailed~~ in section 2.1.3, stalagmite Mg/Ca ratios ~~might also~~ provide some useful  
252 **corroborative** information ~~to test the robustness of the reconstructed rainfall record as~~  
253 ~~well.~~

254 Stalagmite Mg/Ca ratio is ~~another~~ proxy mainly controlled by local rainfall **with**  
255 **higher Mg/Ca values corresponding to lower rainfall** (Fairchild and Treble, 2009),  
256 though it may show some temperature dependence, increasing slightly with  
257 temperature ~~raise~~ **increase**, ~~higher Mg/Ca values usually correspond to lower rainfall~~  
258 ~~(Fairchild and Treble, 2009).~~ **This** ~~The~~ **variation** is understood to result from CO<sub>2</sub>-  
259 degassing occurring earlier during water movement in dry seasons as cave water seeps  
260 more slowly, thus Ca is lost from karst waters by formation of calcite earlier during  
261 transport processes and before waters reach the stalagmite. Such a prior-calcite-  
262 precipitation process would be expected to produce higher Mg/Ca ratios (Tremaine  
263 and Froelich, 2013; Fairchild and Treble, 2009). Although it is hard to obtain  
264 quantitative rainfall data from Mg/Ca ratios, the ~~change~~ **variation** of Mg/Ca may give  
265 a qualitative indication of ~~the~~ rainfall variability and trend. Therefore the variation  
266 ~~trend~~ of Mg/Ca ratios could ~~tell~~ **indicate** whether the reconstructed rainfall from  
267  $\Delta\delta^{18}\text{O}$  is reliable or not.

268 The HS4 Mg/Ca sequence presented as a 10-yr moving average record during the  
269 8.2 ka BP event is shown in Fig. 32c. As high Mg/Ca values are considered to indicate  
270 low rainfall, the Y axis of Mg/Ca was reversed to make the comparison clearer. Both  
271 the Mg/Ca ratios and the reconstructed rainfall data are presented as 10-yr moving  
272 average values. Although the two data sets show slight differences, there is a general  
273 inverse relationship between the two sequences giving a correlation coefficient ( $R^2$ ) of  
274 0.56 (n=219). And overall similarity could be observed between the trends of the two  
275 patterns with high (low) Mg/Ca values corresponding to low (high) rainfall, which  
276 suggests that the Mg/Ca results ~~roughly~~ **generally** support the reconstructed rainfall  
277 record ~~as well.~~

278 The reconstructed rainfall record (Fig.32b) shows a maximum decline in annual  
279 rainfall of 350 mm/yr, which is nearly twice that obtained from the low-resolution  
280 (~100-yr) rainfall record (Hu et al., 2008a) during the same period and the lowest  
281 annual rainfall in this study is lower than that from Hu et al. (2008a) by ~100 mm.  
282 This is believed to be a result of the record resolution. Fig.32b also shows that the  
283 period of decreasing rainfall at the beginning of the event lasts for ~70 years, before  
284 entering into an extreme dry period. During the central period of the 8.2 ka BP event,



285 the average annual rainfall is only ~1200 mm, which appears to be the driest period  
286 during the whole Holocene in this area, lasting for ~50 years. ~~As-t~~The rainfall  
287 calculation developed in Hu et al. (2008a) was made by averaging annual rainfall  
288 records from 6 sites between Heshang and Dongge(Fig. 1) and the averaged annual  
289 rainfall between 1950 and 1990 from the 6 sites is ~1380 mm, indicating the average  
290 annual rainfall during the central 8.2 ka BP period is less than present by ~200 mm.

#### 291 4 Discussions

292 It has been reported that the response of the EAMA to North Atlantic cooling during  
293 the 8.2 ka BP event results from atmospheric rather than oceanic processes (Liu et al.,  
294 2013). It might be assumed that the high northern latitude ice-cover reinforces  
295 Northern Hemisphere cooling, increasing the temperature gradient between the high  
296 and low latitudes which leads to southward migration of the inter-tropical  
297 convergence zone (Chiang and Bitz, 2005; Broccoli et al., 2006). This would result in  
298 weakening of the East Asian Monsoon and increased aridity-around. Assessment of  
299 the sensitivity of southwest China climate response to North Atlantic cooling might  
300 provide a clue to how North Atlantic cooling affects the EAMA.

301 Fig. 45 demonstrates three sequences of Greenland ice core  $\delta^{18}\text{O}$  (Thomas et al.,  
302 2007)(Fig. 45a) , a palaeo-temperature indicator (Stuiver, et al., 1995), Greenland ice  
303 core  $\delta^{15}\text{N}$  (Kobashi et al., 2007)(Fig. 45b), a newly developed palaeo-temperature  
304 proxy (Buizert et al., 2014) and the reconstructed rainfall record in southwest China  
305 during the 8.2 ka BP period(Fig. 45c). The data shown in Fig. 45a are from Thomas et  
306 al. (2007) with a 3-yr resolution. To allow comparison with the reconstructed rainfall  
307 records, the  $\delta^{18}\text{O}$  of the ice core was processed to provide a 10-yr moving average  
308 ~~sequence~~. The  $\delta^{15}\text{N}$  data in Fig. 45b are from Kobashi et al. (2007) with a 11-yr  
309 resolution and were processed similarly.

310 As low Greenland ice  $\delta^{18}\text{O}$  and  $\delta^{15}\text{N}$  values indicate local cooling (Thomas et al.,  
311 2007; Kobashi et al., 2007), both Fig. 45a and Fig. 45b reveal similar trends of  
312 decreasing temperature during the 8.2 ka BP event. The comparison between each  
313 data set in Fig.45 suggests that the decrease in rainfall in southwest China may indeed  
314 be in response to Greenland cooling. Further analysis shows a ~~slight positive-weak~~  
315 correlation between Greenland ice core  $\delta^{18}\text{O}$  and the reconstructed rainfall with a  
316 correlation coefficient ( $R^2$ ) of 0.47 (n=219) indicating a 1‰ drop in Greenland ice  
317 core  $\delta^{18}\text{O}$  could lead to ~7% decrease in rainfall in southwest China. Though there is  
318 not enough  $\delta^{15}\text{N}$  data to reveal further correlations, it does indicate a drop of  $3.3 \pm 1^\circ\text{C}$   
319 when the 8.2 ka BP event occurred(Kobashi et al., 2007). As the reconstructed annual  
320 rainfall record reveals a maximum decrease of 350 mm, the magnitude of rainfall  
321 response of southwest China to Greenland cooling during 8.2 ka BP period could be  
322 assessed as  $110 \pm 30 \text{ mm}/^\circ\text{C}$ .

#### 323 5 Conclusions

- 324 1. Based on a comparison of two high-resolution stalagmite  $\delta^{18}\text{O}$  records from  
325 Dongge cave and Heshang cave along the monsoon moisture transport  
326 pathway in China, a 10-yr moving average quantitative annual rainfall record  
327 in southwest China is established during the 8.2 ka BP event.
- 328 2. Significant positive correlation between **recent monitored** drip water annual  
329 average  $\delta^{18}\text{O}$  differences from two caves along the monsoon moisture  
330 transport pathway and the regional average annual rainfall from May 2011 to  
331 April 2014 provides ~~a monitoring~~ support for the reconstruction. ~~And s~~ Similar  
332 trends between the reconstructed rainfall ~~sequence~~ and ~~the~~ stalagmite Mg/Ca  
333 ratios, another proxy of rainfall, ~~further~~ increase the confidence of the  
334 quantization of the rainfall record.
- 335 3. The reconstructed rainfall record shows that the annual rainfall in southwest  
336 China decreased sharply by ~350 mm in ~70 years when the 8.2 ka BP event  
337 occurred and experienced an extreme drying period lasting for ~50 years  
338 during the central event. Compared with the modern instrumental records, the  
339 averaged annual rainfall in southwest China during the 8.2 ka BP event is less  
340 than that of present (1950 ~ 1990) by ~200 mm.
- 341 4. ~~The correlation analysis~~ **A comparison** between ~~the~~ reconstructed rainfall in  
342 southwest China and Greenland ice core  $\delta^{18}\text{O}$ , an indicator of temperature,  
343 suggests that the rainfall decrease in southwest China during the 8.2 ka BP  
344 period coupled with Greenland cooling. ~~And a~~ possible response rate of  $110 \pm$   
345  $30 \text{ mm}/^\circ\text{C}$  could be presumed by the temperature drop derived from Greenland  
346 ice core  $\delta^{15}\text{N}$  and rainfall decrease from the reconstructed record.

347 **Acknowledgements.** This work was supported by NSFC Grants 41371216 and  
348 41130207. We thank the editor, **Prof. Dominik Fleitmann**, and the two anonymous  
349 reviewers for their valuable comments that greatly improved the manuscript. **We also**  
350 **thank Dr. Nick Belshaw for proofreading the manuscript.**

## 351 **References**

- 352 Alley, R. B. and Ágústsson, A. M.: The 8k event: cause and consequences of a  
353 major Holocene abrupt climate change, *Quaternary Sci. Rev.*, 24, 1123–1149, 2005.
- 354 Alley, R. B., Mayewski, P. A., Sowers, T., Stuiver, M., Taylor, K. C., and Clark, P. U.:  
355 Holocene climatic instability: A prominent, widespread event 8200 yr ago, *Geology*,  
356 25, 483–486, 1997.
- 357 Broccoli, A. J., Dahl, K. A., and Stouffer, R. J.: Response of the ITCZ to Northern  
358 Hemisphere cooling, *Geophys. Res. Lett.*, 33, L01702, 2006.
- 359 Buizert, C., Gkinis, V., Severinghaus, J. P., He, F., Lecavalier, B. S., Kindler, P.,  
360 Leuenberger, M., Carlson, A. E., Vinther, B., Masson-Delmotte, V., White, J. W. C.,  
361 Liu, Z., Otto-Bliesner, B., and Brook, E. J.: Greenland temperature response to  
362 climate forcing during the last deglaciation, *Science*, 345, 1177–1180, 2014.
- 363 Cheng, H., Fleitmann, D., Edwards, R. L., Wang, X., Cruz, F. W., Auler, A. S.,

364 Mangini, A., Wang, Y., Kong, X., Burns, S. J., and Matter, A.: Timing and structure  
365 of the 8.2 kyr B.P. event inferred from  $\delta^{18}\text{O}$  records of stalagmites from China,  
366 Oman, and Brazil, *Geology*, 37, 1007–1010, 2009.

367 Chiang, J. C. H. and Bitz, C. M.: Influence of high latitude ice cover on the marine  
368 Intertropical Convergence Zone, *Clim. Dynam.*, 25, 477–496, 2005.

369 Condron, A. and Winsor, P.: A subtropical fate awaited freshwater discharged from  
370 glacial Lake Agassiz, *Geophys. Res. Lett.*, 38, L03705, 2011.

371 Daley, T. J., Thomas, E. R., Holmes, J. A., Street-Perrottd, F. A., Chapman, M. R.,  
372 Tindallf, J. C., Valdesf, P. J., Loaderd, N. J., Marshallg, J. D., Wolffb, E. W.,  
373 Hopleyh, P. J., Atkinsonc, T., Barberi, K. E., Fisherg, E. H., Robertsond, I., Hughesi,  
374 P. D. M., and Roberts, C. N.: The 8200 yr BP cold event in stable isotope records  
375 from the North Atlantic region, *Global Planet. Change*, 79, 288–302, 2011.

376 Dayem, K. E., Molnar, P., Battisti, D. S., and Roe, G. H.: Lessons learned from  
377 oxygen isotopes in modern precipitation applied to interpretation of speleothem  
378 records of paleoclimate from eastern Asia, *Earth Planet. Sc. Lett.*, 295, 219–230,  
379 2010.

380 **Ding, Y., Li, C., and Liu, Y.: Overview of the South China Sea Monsoon experiment.**  
381 ***Adv. Atmos. Sci.*, 21, 343–360, 2004.**

382 Dixit, Y., Hodell, D. A., Sinhab, R., and Petrie, C. A.: Abrupt weakening of the Indian  
383 summer monsoon at 8.2 kyr B.P., *Earth Planet. Sc. Lett.*, 391, 16–23, 2014.

384 Domínguez-Villar, D., Fairchild, I. J., Baker, A., Wang, X., Edwards, R. L., and Cheng,  
385 H.: Oxygen isotope precipitation anomaly in the North Atlantic region during the  
386 8.2 ka event, *Geology*, 37, 1095–1098, 2009.

387 Duan, W., Ruan, J., Luo, W., Li, T., Tian, L., Zeng, G., Zhang, D., Bai, Y., Li, J., Tao,  
388 T., Zhang, P., Baker, A., and Tan, M.: The transfer of seasonal isotopic variability  
389 between precipitation and drip water at eight caves in the monsoon regions of  
390 China, *Geochim. Cosmochim. Acta*, 183: 250–266, 2016.

391 Dykoski, C. A., Edwards, R. L., Cheng, H., Yuan, D., Cai, Y., Zhang, M., Lin, Y., Qing,  
392 J., An, Z., and Revenaugh, J.: A high-resolution, absolute dated Holocene and  
393 deglacial Asian monsoon record from Dongge Cave, China, *Earth Planet. Sc. Lett.*,  
394 233, 71–86, 2005.

395 Ellwood, B. B. and Gose, W. A.: Heinrich H1 and 8200 yr B.P. climate events  
396 recorded in Hall’s Cave, Texas, *Geology*, 34, 753–756, 2006.

397 Fairchild, I. J. and Treble, P. C.: Trace elements in speleothems as recorders of  
398 environmental change, *Quaternary Sci. Rev.*, 28, 449–468, 2009.

399 Ge, Q., Chu, F. Y., Xue, Z., Liu, J. P., Du, Y., and Fang, Y.: Paleoenvironmental  
400 records from the northern South China Sea since the Last Glacial Maximum, *Acta*  
401 *Oceanol. Sin.*, 29, 46–62, 2010.

402 Hede, M. U., Rasmussen, P., Noe-Nygaard, N., Clarke, A. L., Vinebrooke, R. D., and  
403 Olsen, J.: Multiproxy evidence for terrestrial and aquatic ecosystem responses  
404 during the 8.2 ka cold event as recorded at Højby Sø, Denmark, *Quaternary Res.*,  
405 73, 485–496, 2010.

406 Hong, Y. T., Hong, B., Lin, Q. H., Shibatab, Y., Zhua, Y. X., Lengc, X. T., and Wang,  
407 Y.: Synchronous climate anomalies in the western North Pacific and North Atlantic  
408 regions during the last 14,000 years, *Quaternary Sci. Rev.*, 28, 840–849, 2009.

409 Hu, C., Henderson, G. M., Huang, J., Xie, S., Sun, Y., and Johnson K. R.:  
410 Quantification of Holocene Asian monsoon rainfall from spatially separated cave  
411 records, *Earth Planet. Sc. Lett.*, 266, 221–232, 2008a.

412 Hu, C., Henderson, G. M., Huang, J., Chen, Z., and Johnson, K. R.: Report of a three-  
413 year monitoring programme at Heshang Cave, Central China, *Int. J. Speleol.*, 37 :  
414 143–151, 2008b.

415 Khasnis, A. A. and Nettleman, M. D.: Global warming and infectious disease, *Arch.*  
416 *Med. Res.*, 36, 689–696, 2005.

417 Kobashi, T., Severinghaus, J. P., Brook, E. J., Barnola, J. M., and Grachev, A. M.:  
418 Precise timing and characterization of abrupt climate change 8200 years ago from  
419 air trapped in polar ice, *Quaternary Sci. Rev.*, 26, 1212–1222, 2007.

420 LeGrande A. N. and Schmidt G. A.: Ensemble, water isotope-enabled, coupled  
421 general circulation modeling insights into the 8.2 ka event, *Paleoceanography*, 23,  
422 PA3207, 2008.

423 Liu, Y., Henderson, G. M., Hu, C., Mason, A. J. Charnley, N., Johnson, K. R., and Xie,  
424 S.: Links between the East Asian monsoon and North Atlantic climate during the  
425 8,200 year event, *Nat. Geosci.*, 6, 117–120, 2013.

426 Liu, Z., Wen, X., Brady, E.C., Otto-Bliesner, B., Yu, G. , Lu, H., Cheng, H., Wang, Y.,  
427 Zheng, W., Ding, Y., Edwards, R.L., Cheng, J., Liu, W., and Yang, H.: Chinese cave  
428 records and the East Asia Summer Monsoon, *Quaternary Sci. Rev.*, 83, 115-128,  
429 2014.

430 Ljung, K., Björck, S., Renssen, H., and Hammarlund, D.: South Atlantic island record  
431 reveals a South Atlantic response to the 8.2 kyr event, *Clim. Past*, 4, 35–45, 2008.

432 Martrat, B., Grimalt, J. O., Lopez-Martine, C., Cacho, I., Sierro, F. J., Flores, J. A.,  
433 Zahn, R., Canals, M., Curtis, J. H., and Hodell, D. A.: Abrupt temperature changes  
434 in the western Mediterranean over the past 250,000 years, *Science*, 306, 1762–1765,  
435 2004.

436 Mischke, S. and Zhang, C. J.: Holocene cold events on the Tibetan Plateau, *Global*  
437 *Planet. Change*, 72, 155–163, 2010.

438 Morrill C., Anderson, D. M., Bauer, B. A., Buckner, R., Gille, E. P., Gross, W. S.,  
439 Hartman, M., and Shah, A.: Proxy benchmarks for intercomparison of 8.2 ka  
440 simulations, *Clim. Past*, 9, 423–432, 2013.

441 Morrill, C., Wagner, A. J., Otto-Bliesner, B. L., and Rosenbloom, N.: Evidence for  
442 significant climate impacts in monsoonal Asia at 8.2 ka from multiple proxies and  
443 model simulations, *J. Earth Environ.*, 2, 426–441, 2011.

444 Pall, P., Allen, M. R., and Stone, D. A.: Testing the Clausius–Clapeyron constraint on  
445 changes in extreme precipitation under CO<sub>2</sub> warming, *Clim. Dynam*, 28, 351–363,  
446 2007.

447 Prasad, S., Witt, A., Kienel, U., Dulski, P., Bauer, E., and Yancheva, G.: The 8.2 ka

448 event: Evidence for seasonal differences and the rate of climate change in western  
449 Europe, *Global Planet. Change*, 67, 218–226, 2009.

450 Rahmstorf, S.: A semi-empirical approach to projecting future sea-level rise, *Science*,  
451 315, 368–370, 2007.

452 Snowball, I., Muscheler, R., Zillén, L., Sandgren, P., Stanton, T., and Ljung, K.:  
453 Radiocarbon wiggle matching of Swedish lake varves reveals asynchronous climate  
454 changes around the 8.2 kyr cold event, *Boreas*, 39, 720–733, 2010.

455 Stuiver, M., Grootes, P. M., and Braziunas, T. F.: The GISP2  $\delta^{18}\text{O}$  record of the past  
456 16,500 years and the role of the Sun, ocean and volcanoes, *Quaternary Res.*, 44,  
457 341–354, 1995.

458 Szeroczyńska, K. and Zawisza, E.: Records of the 8200 cal BP cold event reflected in  
459 the composition of subfossil Cladocera in the sediments of three lakes in Poland,  
460 *Quatern. Int.*, 233, 185–193, 2011.

461 Thomas, E. R., Wolff, E. W., Mulvaney, R., Steffensen, J. P., Johnsen, S. J.,  
462 Arrowsmith, C., White, J. W.C., Vaughn, B., and Popp, T.: The 8.2 ka event from  
463 Greenland ice cores, *Quaternary Sci. Rev.*, 26, 70–81, 2007.

464 Tremaine, D. M. and Froelich, P.N.: Speleothem trace element signatures: A  
465 hydrologic geochemical study of modern cave dripwaters and farmed calcite,  
466 *Geochim. Cosmochim. Acta*, 121, 522–545, 2013.

467 Walther, G. R., Post, E., Convey, P., Menzel, A., Parmesan, C., Beebee, T. J. C.,  
468 Fromentin, J. M., Hoegh-Guldberg, O., and Bairlein, F.: Ecological responses to  
469 recent climate change, *Nature*, 416, 389–395, 2002.

470 Wang, Y., Cheng, H., Edwards, R. L., He, Y., Kong, X., An, Z., Wu, J., Kelly, M. J.,  
471 Dykoski, C. A., and Li, X.: The Holocene Asian Monsoon: links to solar changes  
472 and North Atlantic climate, *Science*, 308, 854–857, 2005.

473 Wu, J., Wang, Y., Cheng, H., Kong, X., and Liu, D.: Stable isotope and trace element  
474 investigation of two contemporaneous annually-laminated stalagmites from  
475 northeastern China surrounding the “8.2 ka event”, *Clim. Past*, 8, 1497–1507, 2012.

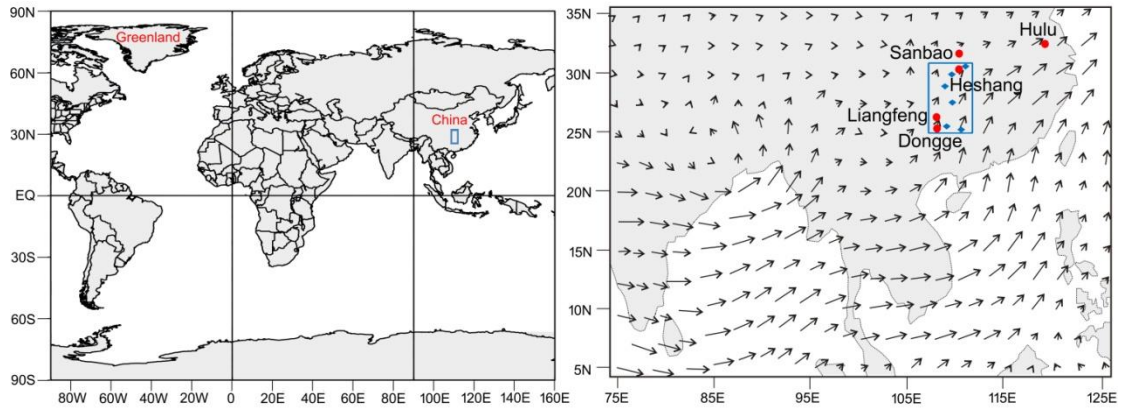
476 Yu, X., Zhou, W., Franzen, L. G., Feng, X., Peng, C., and Jull, A. J. T.: High-  
477 resolution peat records for Holocene monsoon history in the eastern Tibetan Plateau,  
478 *Sci. China Earth Sci.*, 49, 615–621, 2006.

479 Zeng, G., Luo, W., Wang, S., and Du, X.: Hydrogeochemical and climatic  
480 interpretations of isotopic signals from precipitation to drip waters in Liangfeng  
481 Cave, Guizhou Province, China, *Environ. Earth Sci.*, 74, 1509–1519, 2015.

482 Zheng, Y., Zhou, W., Xie, S., and Yu, X.: A comparative study of n-alkane biomarker  
483 and pollen records: an example from southern China, *Chinese Sci. Bull.*, 54, 1065–  
484 1072, 2009.

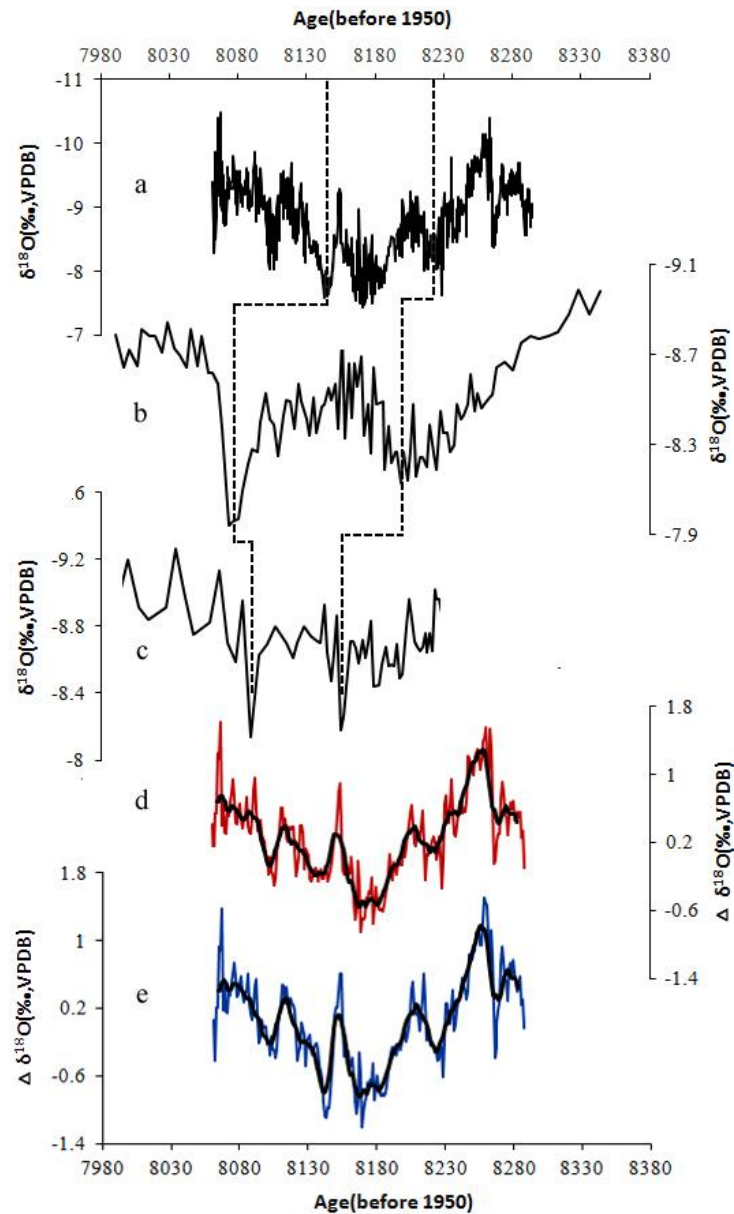
485 Zheng, Y., Kissel, C., Zheng, H., Lajb, C., and Wang, K.: Sedimentation on the inner  
486 shelf of the East China Sea: Magnetic properties, diagenesis and paleoclimate  
487 implications, *Mar. Geol.*, 268, 34–42, 2010.





488

489 Figure 1. Location maps. The left map shows the location of Greenland and southwest China (blue  
 490 box). The right map shows the location of Heshang cave and other Chinese caves (red points), with  
 491 main feature of the summer monsoon marked. Smaller arrows reflect moisture transport and  
 492 direction averaged over the whole atmosphere (Ding et al., 2004). The blue box indicates the  
 493 specific region for which comparison of Heshang and Dongge allows rainfall reconstruction, and  
 494 the blue diamond patterns show the location of six modern rainfall stations detailed in Hu et  
 495 al.(2008) .



496

497

498

499

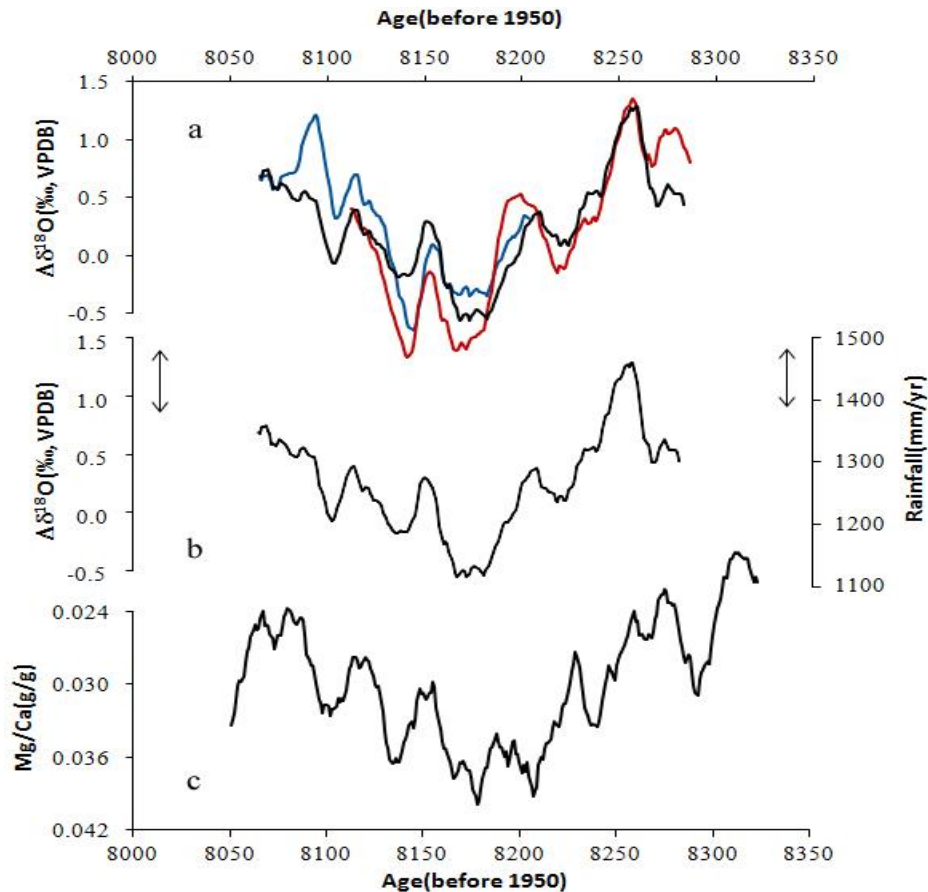
500

501

502

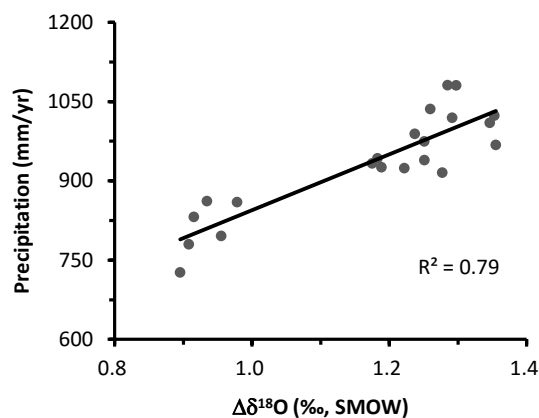
503

Figure 24. Original  $\delta^{18}\text{O}$  stalagmite records adopted in this paper displayed with  $\Delta\delta^{18}\text{O}$  sequences between stalagmites from Dongge and Heshang. a. HS4  $\delta^{18}\text{O}$  record from Heshang cave(Liu et al., 2013); b. DA  $\delta^{18}\text{O}$  record from Dongge cave(Cheng et al., 2009); c. D4  $\delta^{18}\text{O}$  record from Dongge cave (Cheng et al., 2009); d.  $\Delta\delta^{18}\text{O}$  between DA and HS4 (red) with a 10-year moving average(black); e.  $\Delta\delta^{18}\text{O}$  between D4 and HS4 (blue) with a 10-year moving average (black). The dashed lines show matched typical corresponding peaks from each original record.



504

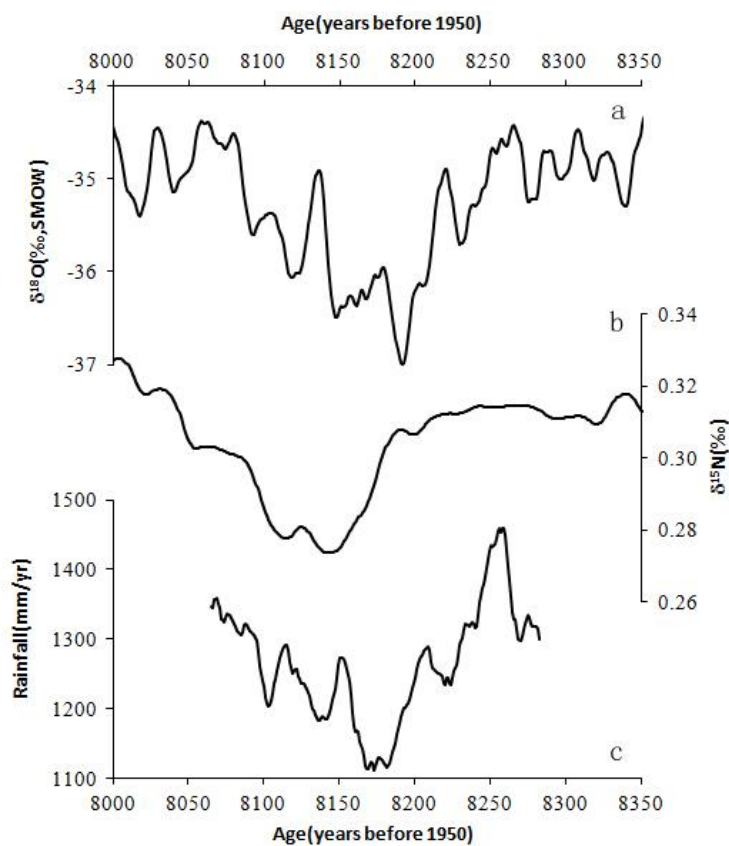
505 Figure 32. 10-yr moving average records during the 8.2 ka BP period. a).  $\Delta \delta^{18}\text{O}$  records  
 506 between HS4 and DA with unchanged chronology (black), shifting DA 50-yr younger (blue)  
 507 and 50-yr older (red); b).  $\Delta \delta^{18}\text{O}$  record between HS4 and DA and reconstructed annual rainfall  
 508 in southwest China with error bars indicated; c). Mg/Ca ratios of HS4 shown on inverted scales,  
 509 which reveals a similar trend to the rainfall sequence, increasing the confidence of the  
 510 quantization of the reconstructed record.



511

512 Figure 43. Correlation analysis between mean annual moving average precipitation and drip  
 513 water  $\delta^{18}\text{O}$  difference of from 2-month delayed LF6 and 4-month delayed HS4 from May  
 514 2011 to April 2014. The  $\Delta \delta^{18}\text{O}$  data are calculated from monthly monitoring data from  
 515 Liangfeng cave and Heshang cave (Duan et al., 2016). The annual precipitation data are the  
 516 average from six sites between Dongge cave and Heshang cave mentioned-detailed in Hu et al.

517 (2008a) and the original monthly rainfall data are from [http://www.wunderground.com/](http://www.wunderground.com/history/)  
 518 history/. The correlation factor of 0.79 indicates a significant positive correlation between  
 519 ~~annual~~-regional **annual** rainfall and annual  $\Delta\delta^{18}\text{O}$ .  
 520



521  
 522 Figure 54. Records from Greenland ice core  $\delta^{18}\text{O}$  (Thomas et al., 2007) (a), Greenland ice core  
 523  $\delta^{15}\text{N}$  (Kobashi et al., 2007) (b) and the reconstructed annual rainfall from this study(c) during  
 524 the 8.2 ka BP event. Three sequences show a similar pattern indicating the decrease in rainfall  
 525 in southwest China **was** coupled with Greenland cooling during the 8.2 ka BP event.  
 526